

Constraining Emission Estimates of CFC-11 in Eastern China Based on Local Observations at Surface Stations and Mount Tai

Xiaoqing Huang, Yanli Zhang,* Likun Xue, Jianhui Tang, Wei Song, Donald R. Blake, and Xinming Wang*



Cite This: *Environ. Sci. Technol. Lett.* 2021, 8, 940–946



Read Online

ACCESS |



Metrics & More

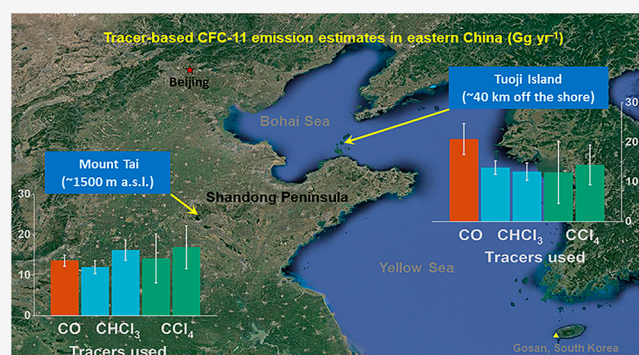


Article Recommendations



Supporting Information

ABSTRACT: While observations at global background sites in east Asia suggested unexpectedly increased emissions of trichlorofluoromethane (CFC-11) after 2012 in eastern China, particularly in Shandong province, there is a lack of local monitoring data to constrain the emission estimates. Here we report observations of ambient CFC-11 during 2012–2018 in Shandong province at five sites, including three rural sites and two background sites [one at Tuoji Island (TJI) in the Bohai Sea and the other at Mount Tai (MT), 1534 m above sea level]. The mixing ratios of CFC-11 at rural sites were 17–23% above the global background levels at Mauna Loa, Hawaii, and observations at MT and TJI revealed larger enhancements occurring in air masses traveling through the polyurethane foam industry region of the Shandong Peninsula. On the basis of the ratios of CFC-11 to tracers such as carbon monoxide (CO), chloroform (CHCl₃), and carbon tetrachloride (CCl₄) at the MT and TJI sites, the estimated emissions of CFC-11 in eastern China ranged from 12.0 ± 1.6 to 20.8 ± 3.9 Gg year⁻¹ with an average of 14.7 ± 4.3 Gg year⁻¹ in 2014 and 2017–2018. These tracer-based estimates may represent the upper limits due to relatively higher ratios of CFC-11 to tracers in the hot spot province.



INTRODUCTION

Chlorofluorocarbons (CFCs), as the first generation of ozone-depleting substances (ODSs), contribute the most to stratospheric reactive chlorine that can effectively damage the ozone layer.¹ The production and consumption of trichlorofluoromethane (CFC-11, CFCl₃), the second most abundant CFC in the atmosphere, were scheduled to be phased out in non-Article 5 countries by 1996 and in Article 5 countries (mostly developing countries, including China) by 2010 under the Montreal Protocol and its Amendments,² and as expected, the atmospheric abundance of CFC-11 has been decreasing at an accelerating rate since the mid-1990s.^{3,4} However, recent studies revealed a slowdown in its decline, indicative of an increase in the emission of CFC-11 since 2012.^{4,5} Inverse modeling results based on observations at Gosan, South Korea, and Hateruma, Japan, suggested CFC-11 emissions of 13.4 ± 1.7 Gg year⁻¹ from eastern China in 2014–2017;⁶ however, the estimated emissions decreased to 5 ± 2 Gg year⁻¹ in eastern China in 2019, and atmospheric mixing ratios of CFC-11 resumed their decline globally.^{7,8} Meanwhile, Adcock et al.¹⁸ derived tracer-based CFC-11 emission estimates ranging from 17 to 22 Gg year⁻¹ in eastern mainland China with an average of 19 ± 6 Gg year⁻¹ based on air samples collected with canisters during 2014–2018 in Taiwan. Due to a lifetime of ~52 years for CFC-11,¹⁴ the delay in the ozone recovery caused by its increased emissions

even for a short period will be of great concern.^{15–17} Therefore, it is vital to have an accurate estimate of the scale of any unexpected emissions.

CFC-11 had been used primarily as a refrigerant and foam blowing agent and was supposed to be released from banks such as air conditioners or foams only after its complete phase-out.^{2,9} The emissions of CFC-11 that were far from what was expected from banks^{10,11} were found to be largely or entirely attributed to the rigid polyurethane (PU) foam industry,^{12,13} with CFC-11 emission either from the foaming process or from rigid polyurethane foams being a significant portion of the CFC-11 bank.⁹ Faced with the CFC-11 crisis in eastern China and the differences in emission estimates of CFC-11 based on observations outside mainland China, we thought it would be better to have local monitoring data to confirm and constrain the estimated emissions, yet data about ambient CFC-11 in mainland China in recent decades are quite sparse,^{19–25} particularly after 2012 in eastern China. As Shandong and

Received: July 7, 2021

Revised: October 2, 2021

Accepted: October 4, 2021

Published: October 7, 2021



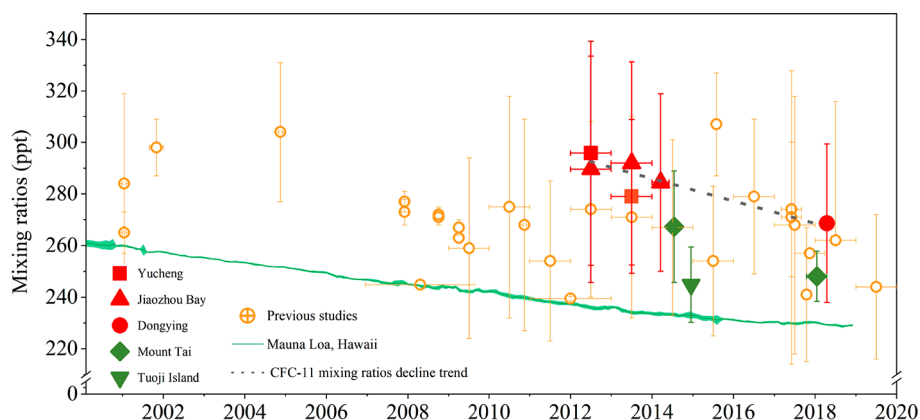


Figure 1. CFC-11 mixing ratios from this study and those reported in China from previous studies^{19–22,24,25,28,29,39–43} (Table S3): empty symbols, CFC-11 mixing ratios reported in previous studies; filled symbols, CFC-11 mixing ratios measured in this study; horizontal error bars, sampling duration for each study; vertical solid line, standard deviation of CFC-11 mixing ratios; light green solid line, CFC-11 mixing ratios from 2000 to 2018 at Mauna Loa Observatory (MLO) in the NOAA monitoring network; light green shaded area, standard deviation of CFC-11 mixing ratios at MLO; gray dashed line, declining trend ($-3.8 \text{ ppt year}^{-1}$) for observed CFC-11 mixing ratios in Shandong.

Hebei provinces of China are suggested to be major regions with increased emissions of CFC-11 in eastern mainland China,⁶ in this study we present field observation data from five campaigns carried out from 2012 to 2018 in Shandong province and estimate CFC-11 emissions in eastern mainland China on the basis of these observations.

MATERIALS AND METHODS

Field Sampling. The field campaigns were carried out at five sites in Shandong province, including three rural sites (Yucheng, YC; Jiaozhou Bay, JZB; and Dongying, DY) and two background sites (Tuoji Island, TJI; and Mount Tai, MT). TJI is approximately 40 km from the shore of Bohai Bay, and the site MT is $\sim 1534 \text{ m}$ above sea level (a.s.l.) (Figure S1). The TJI and MT sites are far from anthropogenic emission sources and can serve as good receptors with better horizontal or vertical mixing of different emission sources (see Figure S2 for air mass footprint). Campaign I was carried out at YC and JZB with samples collected once a week during 2012–2014. Campaigns II and III were conducted at background sites in TJI in winter (four samples daily) and MT in summer (three samples daily) in 2014, respectively. Campaign IV was conducted in the spring of 2018 at DY (six samples daily). For campaign V at MT, two samples were collected every day in the winter of 2017 while four samples were collected every day in the spring of 2018. A detailed description of the sampling sites can be found in previous studies,^{21,24,26,27} and more information about field sampling is presented in Table S1.

All of the ambient samples were collected using cleaned and evacuated 2 L electropolished stainless steel canisters and then sent to the laboratories of the Guangzhou Institute of Geochemistry, Chinese Academy of Sciences (GIG, CAS), and the University of California, Irvine (UCI), for analysis (Table S2).

Laboratory Analysis. Samples sent to GIG were analyzed using a model 7100 preconcentrator (Entech Instruments Inc.) coupled to a gas chromatography-mass spectrometer detector/flame ionization detector/electron capture detector system (GC-MSD/FID/ECD, Agilent Technologies). A detailed description of the analysis can be found in previous studies^{28,29} and Text S1. CFC-11, dichlorodifluoromethane (CFC-12, CF_2Cl_2), chlorodifluoromethane (HCFC-22, CHClF_2), chloro-

form (CHCl_3), methylene dichloride (CH_2Cl_2), and carbon tetrachloride (CCl_4) were determined with MSD by target ions at m/z 103/101, 85/87, 51/67, 83/85, 49/84, and 117/119, respectively. CO was analyzed by a gas chromatography-flame ionization detector system (GC-FID, Agilent Technologies) with a packed column after conversion to CH_4 by a Ni-based catalyst.²⁹ The determination of VOC mixing ratios by the Rowland/Blake group at UCI has been described elsewhere.^{30,31}

Backward Trajectories. One hundred twenty hour backward trajectories for air masses arriving at the two background sites, TJI and MT, at a height of 300 m a.s.l. and 1500 m above ground level, respectively, were calculated using the Hybrid Single-Particle Lagrangian Integrated Trajectory Model (HYSPPLIT) developed by the National Oceanic and Atmospheric Administration (NOAA) Air Resources Laboratory (<http://www.arl.noaa.gov/ready/hysplit4.html>, last accessed October 25, 2020). Meteorological data were obtained from the Global Data Assimilation System (GDAS) data set (3 h and 1 °C resolution, <https://www.ready.noaa.gov/archives.php>). For further cluster analysis, adjacent trajectories were merged into clusters and presented as their mean trajectory (detailed description in Text S2).^{32,33}

Emission Estimates. Emissions of CFC-11 can be derived from its enhanced mixing ratio versus that of a tracer,^{34–37} which should show a significant correlation with CFC-11 and has known emissions.^{18,37,38} The background levels of CFC-11 and tracers in this study are defined as their lowest 25th percentiles.^{29,38} $\Delta\text{CFC-11}$ and Δtracer were obtained by subtracting the background levels from their mixing ratios. The CFC-11 emission, $E_{\text{CFC-11}}$, can be estimated via

$$E_{\text{CFC-11}} = E_{\text{tracer}} S \frac{M_{\text{CFC-11}}}{M_{\text{tracer}}}$$

where E_{tracer} (gigagrams per year) is the emission of the tracer, $M_{\text{CFC-11}}$ and M_{tracer} are the molecular weights of CFC-11 and the tracer, respectively, and S is the slope (parts per trillion/parts per trillion) of the linear correlation (Pearson's) between $\Delta\text{CFC-11}$ and Δtracer . The uncertainty in $E_{\text{CFC-11}}$ from the above equation can be calculated via

$$\sigma_{\text{CFC-11}} = \sqrt{(\sigma_{E_{\text{tracer}}})^2 S^2 + E_{\text{tracer}}^2 \sigma_S^2} \times \frac{M_{\text{CFC-11}}}{M_{\text{tracer}}}$$

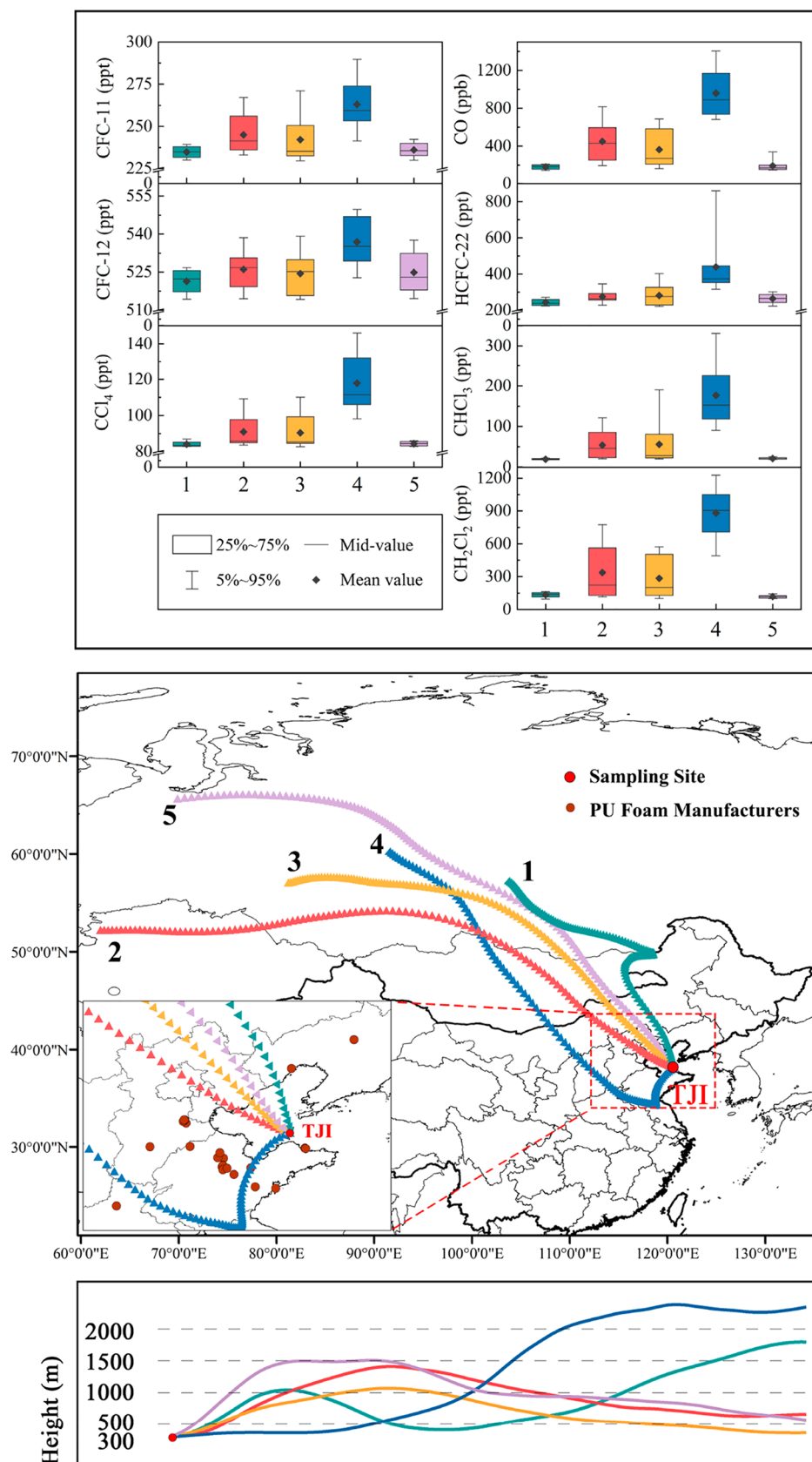


Figure 2. Clustering of air masses arriving at Tuoji Island (TJI) based on 120 h HYSPLIT backward trajectories and the mixing ratios of CFC-11, CO, and halocarbons (CFC-12, HCFC-22, CH₂Cl₂, CHCl₃, and CCl₄) in each cluster.

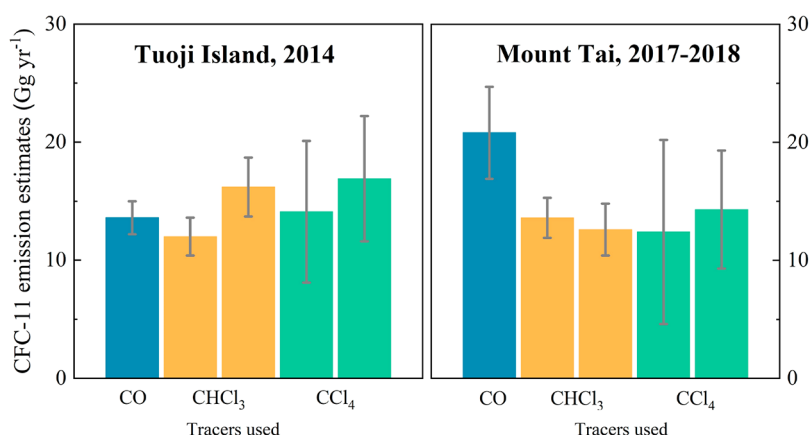


Figure 3. CFC-11 emissions in eastern China estimated on the basis of interspecies correlations between CFC-11 and tracers such as CO (emissions are from the MEIC inventory and ref 46), CHCl₃ (emissions are from different inverse results in ref 47), and CCl₄ (emissions are from different inverse results in ref 48) (gray lines are standard deviations).

where $\sigma_{\text{CFC-11}}$, σ_{Tracer} , and σ_S are the uncertainties in the estimated emissions of CFC-11, the emissions of tracers, and the $\Delta\text{CFC-11}/\Delta\text{tracer}$ slope S , respectively.

RESULTS AND DISCUSSION

Mixing Ratios of CFC-11. The average mixing ratios of CFC-11 were 287 ± 38 ppt (mean $\pm \sigma$) at YC (2012–2013), 290 ± 41 ppt at JZB (2012–2014), and 269 ± 31 ppt at DY (March and April 2018), which were approximately 22%, 23%, and 17%, respectively, above those at the northern hemispheric background station at Mauna Loa Observatory (MLO) in Hawaii during the same time spans (Figure S1 and Table S2). At the island site TJI, CFC-11 mixing ratios observed in December 2014 ranged from 230 to 290 ppt with an average of 245 ± 15 ppt, $\sim 5\%$ above that at MLO. At the MT site, mixing ratios of CFC-11 ranged from 234 to 360 ppt with an average of 267 ± 22 ppt ($\sim 15\%$ above that at MLO) during summer 2014 and ranged from 230 to 279 ppt with an average of 249 ± 13 ppt ($\sim 7\%$ above that at MLO) from winter 2017 to spring 2018, consistent with the average of 257 ppt from June 2017 to April 2018 at the same MT site as reported by Yang et al.²⁴ The mixing ratios of CFC-11 as high as 360 ppt at the MT site in this study also indicated occasionally there might be extensive CFC-11 emissions.

The ambient mixing ratios of CFC-11 from previous studies in China are pooled together (Figure 1 and Table S3).^{19–22,24,25,28,29,39–43} They seemed to show a decreasing trend before 2012 in China's megacities, including the Pearl River Delta, Shanghai, and Beijing. However, as reported in recent studies in the North China Plain and in this study, the mixing ratios of CFC-11 seemed to increase to higher levels; CFC-11 mixing ratios as high as 307 ± 20 ppt were observed at the same MT site in 2015.²⁰ Nevertheless, our observation data, including these at YC and JZB sites during 2012–2014 and that at DY site during 2018, together with the results at the same DY site in a previous study in 2017,²¹ still revealed a decreasing trend in CFC-11 mixing ratios in the rural areas of Shandong province at a rate of -3.8 ppt year⁻¹ ($r^2 = 0.84$) during 2012–2018 (Figure 1), faster than those of -1.2 ppt year⁻¹ at MLO from 2012 to 2018 and -0.8 ppt year⁻¹ for the all of China from 2009 to 2019 estimated by Yi et al.²⁵

Emission Source Regions. Air masses arriving at TJI from December 11 to 22, 2014, were clustered into five groups on the

basis of 120 h backward trajectories. Figure 2 presents the mixing ratios of CFC-11, CO, and other halocarbons, including CFC-12, HCFC-22, CH₂Cl₂, CHCl₃, and CCl₄, in each cluster. Cluster 4, traveling from west to east in Shandong province and down to an altitude of 300 m through regions with PU foam industries (Figure S3) before arriving at TJI, showed significantly higher ($p < 0.01$) levels of CFC-11 and other halocarbons than those in the four other clusters with air masses traveling through the Bohai Sea before arriving at TJI. CFC-12 is a byproduct, and CCl₄ is the chemical feedstock for CFC-11 production.^{12,13,44} As shown in Figure S4, stronger correlations between mixing ratios of CFC-11 and CFC-12 were observed for cluster 4 ($r^2 = 0.80$) than for the whole data set ($r^2 = 0.61$). Meanwhile, an increase in the mixing ratios of CCl₄ was also observed during campaign III in 2014 and campaign V in 2017–2018 at the MT site (Figure S5). This is inconsistent with the decreasing trend in its global background values¹ and might also signal possible emissions from illegal CFC-11 production. However, this increase in the mixing ratio of CCl₄ at the high mountain background site MT might be related to other CCl₄-related industrial processes like the production of chloromethanes (CHCl₃ and CH₂Cl₂),^{44,45} the mixing ratios of which also showed an increasing trend (Figure S5). Clusters 2 and 3 with air masses traveling through the Beijing–Tianjin–Hebei region also showed higher mixing ratios of CFC-11 and other halocarbons than clusters 1 and 5 crossing the border of Hebei and Liaoning provinces. At MT, air mass clusters sweeping through lower altitudes (clusters 1, 2, and 4 in Figure S6 and clusters 2 and 3 in Figure S7) showed higher mixing ratios of CFC-11 by >20 ppt, indicating substantial CFC-11 emission sources close to the ground.

Tracer-Based Emission Estimates. CO, HCFC-22, and chloromethanes (CH₂Cl₂, CHCl₃, and CCl₄) are important anthropogenic tracers, of which the chloromethanes are mainly used in industry.^{5,8,18,29} As shown in Figure S9, significant correlations ($p < 0.01$) between CFC-11 and tracers such as CO, CFC-12, HCFC-22, CHCl₃, CH₂Cl₂, and CCl₄ were observed at TJI with good horizontal mixing and at MT with good vertical mixing. The $\Delta\text{CFC-11}/\Delta\text{CO}$ (parts per trillion/parts per billion) slopes at MT were 0.087 in 2014 and 0.079 in 2017–2018, while the slope at TJI was relatively lower (0.039) in December due to a larger amount of CO emission during the regions' heating season. Tracers that have reported emissions in eastern China^{46–48} were chosen for estimating CFC-11

emissions in this region of great concern. CO emissions are obtained from MEIC (Multiresolution Emission Inventory for China, <http://www.meicmodel.org>, last accessed February 15, 2021) and ref 46, and emissions of CHCl₃ and CCl₄ were estimated in previous studies.^{47,48} Table S4 lists available emission estimates of the tracers, the $\Delta\text{CFC-11}/\Delta\text{tracer}$ slopes in this study, and CFC-11 emissions estimates based on the tracer ratio method. The estimated CFC-11 emissions in eastern China in 2014 and 2017–2018 based on different tracers agreed well with each other, ranging from 12.0 ± 1.6 to 20.8 ± 3.9 Gg year⁻¹ with an average of 14.7 ± 4.3 Gg year⁻¹ (Figure 3). This average estimate is comparable to the value of 13.4 ± 1.7 Gg year⁻¹ (Figure S10) from the inverse method for CFC-11 emissions from eastern China based on measurements at Gosan and Hateruma stations⁶ but lower than that of 19 ± 6 Gg year⁻¹ also derived from the tracer ratio method based on observation in Taiwan.¹⁸

It is worth noting that using the tracer ratios in Shandong province to estimate CFC-11 emissions from eastern mainland China will result in an overestimation because Shandong province is a major source region of CFC-11 in eastern China, and the ratios observed in Shandong province would be much higher than that in other regions of eastern China. As an example, the $\Delta\text{CFC-11}/\Delta\text{CO}$ ratio of ~ 0.08 ppt/ppb at MT was even higher than 0.05 ppt/ppb from surface monitoring in 2016 in the PRD region,²³ one of China's most densely populated and highly industrialized regions with stricter control of ODSs.^{21,28} Therefore, the average emission estimate of 14.7 ± 4.3 Gg year⁻¹ from this study based on observations in Shandong province may represent the upper limit of CFC-11 emissions in eastern China, which is quite in line with emission estimates based on measurement at the remote Pacific sites. It is worth noting that observations in this study were still quite discrete and sparse. Although a significant decrease in CFC-11 emissions has been identified since 2019,^{7,8} one big lesson from this CFC-11 crisis is that the unusual emission should have been captured earlier if a network had been established with quality high-time resolution monitoring of these F-gases and inversion modeling for emission estimates. It is time to introduce regular environmental monitoring of these F-gases to ensure implementation of the Montreal Protocol and its amendments in the world's important source areas and fast developing regions.^{49,50}

■ ASSOCIATED CONTENT

SI Supporting Information

The Supporting Information is available free of charge at <https://pubs.acs.org/doi/10.1021/acs.estlett.1c00539>.

Description of sample measurement (Text S1) and cluster analysis (Text S2), distribution of sampling sites and sampling information (Table S1 and Figure S1) and CFC-11 mixing ratios measured at the sites (Figure S1 and Table S2), air mass footprint for TJI and MT sites (Figure S2), distribution of main PU foam manufacturing companies in China (Figure S3 and Table S5), CFC-11 mixing ratios in previous studies (Table S3), correlations between mixing ratios of CFC-11 and CFC-12 for cluster 4 and for the whole data set (Figure S4), comparison of mixing ratios of CHCl₃, CH₂Cl₂, and CCl₄ measured at background sites (Figure S5), clustering of air masses arriving at Mount Tai in 2014 (Figure S6) and in 2017–2018 (Figure S7), air mass trajectory for the highest

mixing ratios of 360 ppt (Figure S8), information for emission estimates of CFC-11 (Table S4), interspecies correlations of CFC-11 with other tracers at background sites (Figure S9), and comparison of CFC-11 emissions in this study with that from previous studies (Figure S10) (PDF)

■ AUTHOR INFORMATION

Corresponding Authors

Xinming Wang – State Key Laboratory of Organic Geochemistry and Guangdong Key Laboratory of Environmental Protection and Resources Utilization, Guangzhou Institute of Geochemistry, Chinese Academy of Sciences, Guangzhou 510640, China; CAS Center for Excellence in Deep Earth Science, Guangzhou 510640, China; University of Chinese Academy of Sciences, Beijing 100049, China; Center for Excellence in Regional Atmospheric Environment, Institute of Urban Environment, Chinese Academy of Sciences, Xiamen 361021, China; orcid.org/0000-0002-1982-0928; Email: wangxm@gig.ac.cn

Yanli Zhang – State Key Laboratory of Organic Geochemistry and Guangdong Key Laboratory of Environmental Protection and Resources Utilization, Guangzhou Institute of Geochemistry, Chinese Academy of Sciences, Guangzhou 510640, China; CAS Center for Excellence in Deep Earth Science, Guangzhou 510640, China; University of Chinese Academy of Sciences, Beijing 100049, China; Center for Excellence in Regional Atmospheric Environment, Institute of Urban Environment, Chinese Academy of Sciences, Xiamen 361021, China; orcid.org/0000-0003-0614-2096; Email: zhang_yl86@gig.ac.cn

Authors

Xiaoqing Huang – State Key Laboratory of Organic Geochemistry and Guangdong Key Laboratory of Environmental Protection and Resources Utilization, Guangzhou Institute of Geochemistry, Chinese Academy of Sciences, Guangzhou 510640, China; CAS Center for Excellence in Deep Earth Science, Guangzhou 510640, China; University of Chinese Academy of Sciences, Beijing 100049, China

Likun Xue – Environment Research Institute, Shandong University, Qingdao 266237, China

Jianhui Tang – Key Laboratory of Coastal Environmental Processes and Ecological Remediation, Yantai Institute of Coastal Zone Research, Chinese Academy of Sciences, Yantai 264003, China; orcid.org/0000-0002-9006-263X

Wei Song – State Key Laboratory of Organic Geochemistry and Guangdong Key Laboratory of Environmental Protection and Resources Utilization, Guangzhou Institute of Geochemistry, Chinese Academy of Sciences, Guangzhou 510640, China; CAS Center for Excellence in Deep Earth Science, Guangzhou 510640, China

Donald R. Blake – Department of Chemistry, University of California, Irvine, California 92697, United States

Complete contact information is available at: <https://pubs.acs.org/doi/10.1021/acs.estlett.1c00539>

Author Contributions

X.H. analyzed data and wrote the paper. Y.Z. and X.W. designed the research and reviewed and revised the paper. L.X., J.T., and

D.R.B. shared their ideas. L.X. and J.T. provided air samples and sampling site information.

Notes

The authors declare no competing financial interest. The data sets used in the study can be accessed from Web sites listed in the references or by contacting the corresponding authors. All data are available at Zenodo (<https://zenodo.org/record/5181531#YRQDVIUzapo>).

ACKNOWLEDGMENTS

This work was supported by the National Natural Science Foundation of China (42022023, 41303078, and 41961144029), the Chinese Academy of Sciences (XDA23010303 and XDA23020301), the Youth Innovation Promotion Association of the Chinese Academy of Sciences (2017406), and the Department of Science and Technology of Guangdong (2020B1212060053).

REFERENCES

- (1) Engel, A.; Rigby, M.; Burkholder, J. B.; Fernandez, R. P.; Froidevaux, L.; Hall, B. D.; Hossaini, R.; Saito, T.; Vollmer, M. K.; Yao, B. Update on ozone-depleting substances (ODSs) and other gases of interest to the Montreal Protocol. In *Scientific Assessment of Ozone Depletion: 2018*; Global Ozone Research and Monitoring Project, Report 58; World Meteorological Organization: Geneva, 2018; Chapter 1.
- (2) United Nations Environmental Programme. Handbook for the Montreal Protocol on Substances that Deplete the Ozone Layer. 2020 (<https://ozone.unep.org/sites/default/files/Handbooks/MP-Handbook-2020-English.pdf>, last accessed 2021-05-05).
- (3) Prinn, R. G.; Weiss, R. F.; Fraser, P. J.; Simmonds, P. G.; Cunnold, D. M.; Aleya, F. N.; O'Doherty, S.; Salameh, P.; Miller, B. R.; Huang, J.; Wang, R. H. J.; Hartley, D. E.; Harth, C.; Steele, L. P.; Sturrock, G.; Midgley, P. M.; McCulloch, A. A history of chemically and radiatively important gases in air deduced from ALE/GAGE/AGAGE. *J. Geophys. Res.-Atmos.* **2000**, *105* (D14), 17751–17792.
- (4) Prinn, R. G.; Weiss, R. F.; Arduini, J.; Arnold, T.; DeWitt, H. L.; Fraser, P. J.; Ganesan, A. L.; Gasore, J.; Harth, C. M.; Hermansen, O.; Kim, J.; Krummel, P. B.; Li, S.; Loh, Z. M.; Lunder, C. R.; Maione, M.; Manning, A. J.; Miller, B. R.; Mitrevski, B.; Muehle, J.; O'Doherty, S.; Park, S.; Reimann, S.; Rigby, M.; Saito, T.; Salameh, P. K.; Schmidt, R.; Simmonds, P. G.; Steele, L. P.; Vollmer, M. K.; Wang, R. H.; Yao, B.; Yokouchi, Y.; Young, D.; Zhou, L. History of chemically and radiatively important atmospheric gases from the Advanced Global Atmospheric Gases Experiment (AGAGE). *Earth Syst. Sci. Data* **2018**, *10* (2), 985–1018.
- (5) Montzka, S. A.; Dutton, G. S.; Yu, P.; Ray, E.; Portmann, R. W.; Daniel, J. S.; Kuijpers, L.; Hall, B. D.; Mondeel, D.; Siso, C.; Nance, D.; Rigby, M.; Manning, A. J.; Hu, L.; Moore, F.; Miller, B. R.; Elkins, J. W. An unexpected and persistent increase in global emissions of ozone-depleting CFC-11. *Nature* **2018**, *557* (7705), 413–417.
- (6) Rigby, M.; Park, S.; Saito, T.; Western, L. M.; Redington, A. L.; Fang, X.; Henne, S.; Manning, A. J.; Prinn, R. G.; Dutton, G. S.; Fraser, P. J.; Ganesan, A. L.; Hall, B. D.; Harth, C. M.; Kim, J.; Kim, K. R.; Krummel, P. B.; Lee, T.; Li, S.; Liang, Q.; Lunt, M. F.; Montzka, S. A.; Muhle, J.; O'Doherty, S.; Park, M. K.; Reimann, S.; Salameh, P. K.; Simmonds, P.; Tunnicliffe, R. L.; Weiss, R. F.; Yokouchi, Y.; Young, D. Increase in CFC-11 emissions from eastern China based on atmospheric observations. *Nature* **2019**, *569* (7757), 546–550.
- (7) Montzka, S. A.; Dutton, G. S.; Portmann, R. W.; Chipperfield, M. P.; Davis, S.; Feng, W.; Manning, A. J.; Ray, E.; Rigby, M.; Hall, B. D.; Siso, C.; Nance, J. D.; Krummel, P. B.; Muhle, J.; Young, D.; O'Doherty, S.; Salameh, P. K.; Harth, C. M.; Prinn, R. G.; Weiss, R. F.; Elkins, J. W.; Walter-Terrinoni, H.; Theodoridi, C. A decline in global CFC-11 emissions during 2018–2019. *Nature* **2021**, *590*, 428–432.
- (8) Park, S.; Western, L. M.; Saito, T.; Redington, A. L.; Henne, S.; Fang, X.; Prinn, R. G.; Manning, A. J.; Montzka, S. A.; Fraser, P. J.; Ganesan, A. L.; Harth, C. M.; Kim, J.; Krummel, P. B.; Liang, Q.; Muhle, J.; O'Doherty, S.; Park, M.-K.; Reimann, S.; Salameh, P. K.; Weiss, R. F.; Rigby, M. A decline in emissions of CFC-11 and related chemicals from eastern China. *Nature* **2021**, *590*, 433–437.
- (9) United Nations Environment Programme (UNEP). Report of the Technology and Economic Assessment Panel (TEAP): Decision XXX/3 TEAP task force report on unexpected emissions of CFC-11. 2019 (https://ozone.unep.org/sites/default/files/2020-07/TEAP_Task_Force_Dec_XXX-3_on_Unexpected_CFC-11_Emissions_May_2019.pdf, last accessed 2021-05-05).
- (10) Lickley, M.; Solomon, S.; Fletcher, S.; Velders, G. J. M.; Daniel, J.; Rigby, M.; Montzka, S. A.; Kuijpers, L. J. M.; Stone, K. Quantifying contributions of chlorofluorocarbon banks to emissions and impacts on the ozone layer and climate. *Nat. Commun.* **2020**, *11*, 1380.
- (11) Fang, X.; Ravishankara, A. R.; Velders, G. J. M.; Molina, M. J.; Su, S.; Zhang, J.; Hu, J.; Prinn, R. G. Changes in emissions of ozone-depleting substances from China due to implementation of the Montreal Protocol. *Environ. Sci. Technol.* **2018**, *52* (19), 11359–11366.
- (12) Environmental Investigation Agency (EIA). Blowing it: Illegal production and use of banned CFC-11 in China's foam blowing industry. 2018 (<https://eia-global.org/reports/20180709-blowing-illegal-production-and-use-of-banned-cfc-11-in-chinas-foam-blowing-industry>, last accessed 2021-06-30).
- (13) Environmental Investigation Agency (EIA). Tip of the iceberg: Implications of illegal CFC production and use. 2018 (<https://eia-global.org/reports/20181102-tip-of-the-iceberg>, last accessed 2021-06-30).
- (14) Newman, P. A.; Ko, M. K.; Reimann, S.; Strahan, S. E.; Atlas, E. L.; Burkholder, J. B.; Chipperfield, M.; Engel, A.; Liang, Q.; Plumb, R. A. Lifetimes of stratospheric ozone-depleting substances, their replacements, and related species. *SPARC Report*; 2013; Vol. 6, WCRP-15 (<https://www.sparc-climate.org/publications/sparc-reports/sparc-report-no-6/>, last accessed 2021-06-14).
- (15) Dhomse, S. S.; Feng, W.; Montzka, S. A.; Hossaini, R.; Keeble, J.; Pyle, J. A.; Daniel, J. S.; Chipperfield, M. P. Delay in recovery of the Antarctic ozone hole from unexpected CFC-11 emissions. *Nat. Commun.* **2019**, *10* (1), 5781.
- (16) Fleming, E. L.; Newman, P. A.; Liang, Q.; Daniel, J. S. The impact of continuing CFC-11 emissions on stratospheric ozone. *J. Geophys. Res.-Atmos.* **2020**, *125* (3), No. e2019JD031849.
- (17) Keeble, J.; Abraham, N. L.; Archibald, A. T.; Chipperfield, M. P.; Dhomse, S.; Griffiths, P. T.; Pyle, J. A. Modelling the potential impacts of the recent, unexpected increase in CFC-11 emissions on total column ozone recovery. *Atmos. Chem. Phys.* **2020**, *20* (12), 7153–7166.
- (18) Adcock, K. E.; Ashfold, M. J.; Chou, C. C. K.; Gooch, L. J.; Mohd Hanif, N.; Laube, J. C.; Oram, D. E.; Ou-Yang, C.-F.; Panagi, M.; Sturges, W. T.; Reeves, C. E. Investigation of east Asian emissions of CFC-11 using atmospheric observations in Taiwan. *Environ. Sci. Technol.* **2020**, *54* (7), 3814–3822.
- (19) Zhang, G.; Yao, B.; Vollmer, M. K.; Montzka, S. A.; Mühle, J.; Weiss, R. F.; O'Doherty, S.; Li, Y.; Fang, S.; Reimann, S. Ambient mixing ratios of atmospheric halogenated compounds at five background stations in China. *Atmos. Environ.* **2017**, *160*, 55–69.
- (20) Yang, F.; Wang, Y.; Li, H.; Yang, M.; Li, T.; Cao, F.; Chen, J.; Wang, Z. Influence of cloud/fog on atmospheric VOCs in the free troposphere: a case study at Mount Tai in Eastern China. *Aerosol Air Qual. Res.* **2017**, *17* (10), 2401–2412.
- (21) Zheng, P.; Chen, T.; Dong, C.; Liu, Y.; Li, H.; Han, G.; Sun, J.; Wu, L.; Gao, X.; Wang, X.; Qi, Y.; Zhang, Q.; Wang, W.; Xue, L. Characteristics and sources of halogenated hydrocarbons in the Yellow River Delta region, Northern China. *Atmos. Res.* **2019**, *225*, 70–80.
- (22) Lin, Y.; Gong, D.; Lv, S.; Ding, Y.; Wu, G.; Wang, H.; Li, Y.; Wang, Y.; Zhou, L.; Wang, B. Observations of high levels of ozone-depleting CFC-11 at a remote mountain-top site in Southern China. *Environ. Sci. Technol. Lett.* **2019**, *6* (3), 114–118.
- (23) Zeng, L.; Dang, J.; Guo, H.; Lyu, X.; Simpson, I. J.; Meinardi, S.; Wang, Y.; Zhang, L.; Blake, D. R. Long-term temporal variations and source changes of halocarbons in the Greater Pearl River Delta region, China. *Atmos. Environ.* **2020**, *234*, 117550.

- (24) Yang, M.; Yang, F.; Li, H.; Li, T.; Cao, F.; Nie, X.; Zhen, J.; Li, P.; Wang, Y. CFCs measurements at high altitudes in northern China during 2017–2018: Concentrations and potential emission source regions. *Sci. Total Environ.* **2021**, *754*, 142290.
- (25) Yi, L.; Wu, J.; An, M.; Xu, W.; Fang, X.; Yao, B.; Li, Y.; Gao, D.; Zhao, X.; Hu, J. The atmospheric concentrations and emissions of major halocarbons in China during 2009–2019. *Environ. Pollut.* **2021**, *284*, 117190–117190.
- (26) Yan, W.; Yang, L.; Chen, J.; Wang, X.; Wen, L.; Zhao, T.; Wang, W. Aerosol optical properties at urban and coastal sites in Shandong Province, Northern China. *Atmos. Res.* **2017**, *188*, 39–47.
- (27) Zhang, Y.; Zhang, R.; Yu, J.; Zhang, Z.; Yang, W.; Zhang, H.; Lyu, S.; Wang, Y.; Dai, W.; Wang, Y.; Wang, X. Isoprene mixing ratios measured at twenty sites in China during 2012–2014: comparison with model simulation. *J. Geophys. Res.- Atmos.* **2020**, *125*, No. e2020JD033523.
- (28) Zhang, Y.; Guo, H.; Wang, X.; Simpson, I. J.; Barletta, B.; Blake, D. R.; Meinardi, S.; Rowland, F. S.; Cheng, H.; Saunders, S. M.; Lam, S. H. M. Emission patterns and spatiotemporal variations of halocarbons in the Pearl River Delta region, southern China. *J. Geophys. Res.- Atmos.* **2010**, *115*, D15309.
- (29) Zhang, Y.; Wang, X.; Simpson, I. J.; Barletta, B.; Blake, D. R.; Meinardi, S.; Louie, P. K. K.; Zhao, X.; Shao, M.; Zhong, L.; Wang, B.; Wu, D. Ambient CFCs and HCFC-22 observed concurrently at 84 sites in the Pearl River Delta region during the 2008–2009 grid studies. *J. Geophys. Res.- Atmos.* **2014**, *119* (12), 7699–7717.
- (30) Colman, J. J.; Swanson, A. L.; Meinardi, S.; Sive, B. C.; Blake, D. R.; Rowland, F. S. Description of the analysis of a wide range of volatile organic compounds in whole air samples collected during PEM-Tropics A and B. *Anal. Chem.* **2001**, *73* (15), 3723–3731.
- (31) Simpson, I. J.; Blake, N. J.; Barletta, B.; Diskin, G. S.; Fuelberg, H. E.; Gorham, K.; Huey, L. G.; Meinardi, S.; Rowland, F. S.; Vay, S. A.; Weinheimer, A. J.; Yang, M.; Blake, D. R. Characterization of trace gases measured over Alberta oil sands mining operations: 76 speciated C₂–C₁₀ volatile organic compounds (VOCs), CO₂, CH₄, CO, NO, NO₂, NO_y, O₃, and SO₂. *Atmos. Chem. Phys.* **2010**, *10* (23), 11931–11954.
- (32) Stein, A. F.; Draxler, R. R.; Rolph, G. D.; Stunder, B. J. B.; Cohen, M. D.; Ngan, F. NOAA's HYSPPLIT atmospheric transport and dispersion modeling system. *Bull. Am. Meteorol. Soc.* **2015**, *96* (12), 2059–2077.
- (33) Ding, A. J.; Wang, T.; Fu, C. B. Transport characteristics and origins of carbon monoxide and ozone in Hong Kong, South China. *J. Geophys. Res.- Atmos.* **2013**, *118* (16), 9475–9488.
- (34) Kim, J.; Li, S.; Kim, K. R.; Stohl, A.; Muehle, J.; Kim, S. K.; Park, M. K.; Kang, D. J.; Lee, G.; Harth, C. M.; Salameh, P. K.; Weiss, R. F. Regional atmospheric emissions determined from measurements at Jeju Island, Korea: halogenated compounds from China. *Geophys. Res. Lett.* **2010**, *37*, L12801.
- (35) Li, S.; Kim, J.; Kim, K.-R.; Muehle, J.; Kim, S.-K.; Park, M.-K.; Stohl, A.; Kang, D.-J.; Arnold, T.; Harth, C. M.; Salameh, P. K.; Weiss, R. F. Emissions of halogenated compounds in east Asia determined from measurements at Jeju Island, Korea. *Environ. Sci. Technol.* **2011**, *45* (13), 5668–5675.
- (36) Fang, X.; Wu, J.; Su, S.; Han, J.; Wu, Y.; Shi, Y.; Wan, D.; Sun, X.; Zhang, J.; Hu, J. Estimates of major anthropogenic halocarbon emissions from China based on interspecies correlations. *Atmos. Environ.* **2012**, *62*, 26–33.
- (37) Wang, C.; Shao, M.; Huang, D.; Lu, S.; Zeng, L.; Hu, M.; Zhang, Q. Estimating halocarbon emissions using measured ratio relative to tracers in China. *Atmos. Environ.* **2014**, *89*, 816–826.
- (38) Palmer, P. I.; Jacob, D. J.; Mickley, L. J.; Blake, D. R.; Sachse, G. W.; Fuelberg, H. E.; Kiley, C. M. Eastern Asian emissions of anthropogenic halocarbons deduced from aircraft concentration data. *J. Geophys. Res.- Atmos.* **2003**, *108* (D24), 4753.
- (39) Barletta, B.; Meinardi, S.; Simpson, I. J.; Sherwood Rowland, F.; Chan, C.-Y.; Wang, X.; Zou, S.; Chan, L. Y.; Blake, D. R. Ambient halocarbon mixing ratios in 45 Chinese cities. *Atmos. Environ.* **2006**, *40* (40), 7706–7719.
- (40) Guo, H.; Ding, A. J.; Wang, T.; Simpson, I. J.; Blake, D. R.; Barletta, B.; Meinardi, S.; Rowland, F. S.; Saunders, S. M.; Fu, T. M.; Hung, W. T.; Li, Y. S. Source origins, modeled profiles, and apportionments of halogenated hydrocarbons in the greater Pearl River Delta region, southern China. *J. Geophys. Res.- Atmos.* **2009**, *114*, D11302.
- (41) Shao, M.; Huang, D.; Gu, D.; Lu, S.; Chang, C.; Wang, J. Estimate of anthropogenic halocarbon emission based on measured ratio relative to CO in the Pearl River Delta region, China. *Atmos. Chem. Phys.* **2011**, *11* (10), S011–S025.
- (42) Zhang, F.; Zhou, L.; Yao, B.; Vollmer, M. K.; Grealley, B. R.; Simmonds, P. G.; Reimann, S.; Stordal, F.; Maione, M.; Xu, L.; Zhang, X. Analysis of 3-year observations of CFC-11, CFC-12 and CFC-113 from a semi-rural site in China. *Atmos. Environ.* **2010**, *44* (35), 4454–4462.
- (43) Fang, X.; Wu, J.; Xu, J.; Huang, D.; Shi, Y.; Wan, D.; Wu, H.; Shao, M.; Hu, J. Ambient mixing ratios of chlorofluorocarbons, hydrochlorofluorocarbons and hydrofluorocarbons in 46 Chinese cities. *Atmos. Environ.* **2012**, *54*, 387–392.
- (44) Sherry, D.; McCulloch, A.; Liang, Q.; Reimann, S.; Newman, P. A. Current sources of carbon tetrachloride (CCl₄) in our atmosphere. *Environ. Res. Lett.* **2018**, *13* (2), 024004.
- (45) Park, S.; Li, S. L.; Muhle, J.; O'Doherty, S.; Weiss, R. F.; Fang, X. K.; Reimann, S.; Prinn, R. G. Toward resolving the budget discrepancy of ozone-depleting carbon tetrachloride (CCl₄): an analysis of top-down emissions from China. *Atmos. Chem. Phys.* **2018**, *18* (16), 11729–11738.
- (46) Zheng, B.; Tong, D.; Li, M.; Liu, F.; Hong, C.; Geng, G.; Li, H.; Li, X.; Peng, L.; Qi, J.; Yan, L.; Zhang, Y.; Zhao, H.; Zheng, Y.; He, K.; Zhang, Q. Trends in China's anthropogenic emissions since 2010 as the consequence of clean air actions. *Atmos. Chem. Phys.* **2018**, *18* (19), 14095–14111.
- (47) Fang, X.; Park, S.; Saito, T.; Tunnicliffe, R.; Ganesan, A. L.; Rigby, M.; Li, S.; Yokouchi, Y.; Fraser, P. J.; Harth, C. M.; Krummel, P. B.; Muhle, J.; O'Doherty, S.; Salameh, P. K.; Simmonds, P. G.; Weiss, R. F.; Young, D.; Lunt, M. F.; Manning, A. J.; Gressent, A.; Prinn, R. G. Rapid increase in ozone-depleting chloroform emissions from China. *Nat. Geosci.* **2019**, *12* (2), 89–93.
- (48) Lunt, M. F.; Park, S.; Li, S.; Henne, S.; Manning, A. J.; Ganesan, A. L.; Simpson, I. J.; Blake, D. R.; Liang, Q.; O'Doherty, S.; Harth, C. M.; Muhle, J.; Salameh, P. K.; Weiss, R. F.; Krummel, P. B.; Fraser, P. J.; Prinn, R. G.; Reimann, S.; Rigby, M. Continued emissions of the ozone-depleting substance carbon tetrachloride from eastern Asia. *Geophys. Res. Lett.* **2018**, *45* (20), 11423–11430.
- (49) Solomon, S.; Alcamo, J.; Ravishankara, A. R. Unfinished business after five decades of ozone-layer science and policy. *Nat. Commun.* **2020**, *11*, 4272.
- (50) Weiss, R. F.; Ravishankara, A. R.; Newman, P. A. Huge gaps in detection networks plague emissions monitoring. *Nature* **2021**, *595*, 491–493.